

The Evolution of Barred Spiral Galaxies in the Hubble Deep Fields North and South

R. G. Abraham¹, M. R. Merrifield^{2,3}, R. S. Ellis¹, N. R. Tanvir¹ and J. Brinchmann¹

¹*Institute of Astronomy, University of Cambridge, Madingley Road, Cambridge CB3 0HA*

²*School of Physics & Astronomy, University of Nottingham, Nottingham NG7 2RD*

³*Department of Physics and Astronomy, University of Southampton, SO17 1BJ*

Received: Accepted:

ABSTRACT

The frequency of barred spiral galaxies as a function of redshift contains important information on the gravitational influence of stellar disks in their dark matter halos and also may distinguish between contemporary theories for the origin of galactic bulges. In this paper we present a new quantitative method for determining the strength of barred spiral structure, and verify its robustness to redshift-dependent effects. By combining galaxy samples from the Hubble Deep Field North with newly available data from the Hubble Deep Field South, we are able to define a statistical sample of 18 objectively-defined low-inclination barred spiral systems with $I_{814W} < 23.2$ mag. Analysing the proportion of barred spiral galaxies seen as a function of redshift, we find a significant decline in the barred fraction beyond redshifts $z \simeq 0.5$. The physical significance of this effect remains unclear, but several possibilities include dynamically hotter (or increasingly dark-matter dominated) high-redshift discs, or an enhanced efficiency in bar destruction at high redshifts. By investigating the formation of the “orthogonal” axis of Hubble’s classification tuning fork, our result complements studies of evolution in the early–late sequence, and pushes to later epochs the redshift at which the Hubble classification sequence is observed to be in place.

Key words:

1 INTRODUCTION

Deep exposures with the *Hubble Space Telescope* (HST) and, in particular, those undertaken through the *Hubble Deep Field* (HDF) campaigns (Williams et al 1996), have enabled the study of the morphological evolution of galaxies as a function of redshift (see Ellis 1998 and many references therein). An important goal of such studies is an understanding of the processes by which high redshift systems assemble and become transformed into the population categorised by Hubble’s “tuning fork”. As the deepest exposures reach epochs where the Hubble classification system ceases to provide a useful description of the galaxy population (Abraham et al 1996a), it seems likely that the origin of morphological structure can be understood from detailed analyses of such HST data.

Most morphological studies of faint galaxies have concentrated on addressing the statistics of regular and irregular systems (Glazebrook et al 1995; Abraham et al 1996a,b; Driver et al 1995,1998; Odewahn et al 1996; Schade et al. 1995; Brinchmann et al 1998; Marleau & Simard 1998), either probing for evolution along the early–late sequence of

the tuning fork, or discussing the role of objects best described as altogether outside of the conventional framework of the Hubble sequence. Key questions include the assembly rate of field ellipticals and the evolutionary history of spiral disks. Only recently, through the added signal-to-noise and multi-colour data uniquely available in the HDF exposures, have attempts been made to address possible evolution in *internal* structures of distant galaxies. Such methods are highly appropriate ways of attacking the same questions previously addressed from morphological studies based on the integrated properties of faint galaxies. For example, Abraham et al (1998) examined the homogeneity of internal colours within HDF field ellipticals of known spectroscopic redshift and compared the derived star formation history for field spheroidals with those similarly determined for galactic bulges seen in distant HDF spirals. Provided the various selection effects can be accounted for, such comparisons directly address the question of the order of formation of bulges and stellar disks.

This paper is concerned with extending our earlier HDF study by examining the role that stellar bars play in the evolutionary history of spiral galaxies. Our analysis is moti-

vated by the possibility of an intimate connection between the formation of bars and the growth of galactic bulges. Bar formation can be understood from numerical simulations of self-gravitating disks of stars on circular orbits which are unstable to collapse along one axis (e.g. Miller, Prendergast & Quirk 1970). More recently however, it was discovered that bars are, themselves, unstable: they ultimately buckle perpendicularly to the plane of the disk creating a central spheroidal component similar to a galactic bulge (Combes et al. 1990, Raha et al. 1991). This suggests bulges might form by secular evolution, i.e. through the growth and subsequent collapse of bar instabilities in cold rotating discs. This contrasts with the hitherto established view (Eggen, Lynden-Bell, & Sandage 1962) that galactic bulges form through early dissipationless collapse with discs subsequently growing via gas accretion. An absence of barred spirals at high redshifts would pose serious challenges to secular models.

In addition to understanding the history of bulge formation discussed above, the presence of a bar is an important indicator that the host galaxy has sufficient disk mass (relative to that in the dark halo) for its self-gravity to be important and that the disk material is in well-ordered circular orbits. Accordingly, the frequency of barred galaxies as a function of redshift has important consequences for the proportion of galactic mass contained in dark matter halos as a function of redshift, particularly when combined with kinematic data (Quillen & Sarajedini 1998; Quillen 1998).

Measuring the proportion of barred systems as a function of redshift poses a number of challenges. Simple quantitative measures of bulk galactic structure, such as central concentration or global asymmetry, are adequate for placing galaxies within a one-dimensional early-late classification sequence, but objective measures of finer details of spiral structure are much harder to define and test. Possible evolution in the barred population was claimed on the basis of a visual inspection of galaxies in the northern field of the HDF (hereafter HDF-N) by van den Bergh et al (1996). This observation remains controversial, since bars will, most likely, be harder to detect at rest-frame ultraviolet wavelengths sampled in high redshift ($z > 1$) spirals. van den Bergh et al (1996) considered galaxies at all inclinations to the very limits ($I_{814W} \sim 25$ mag) to which visual morphological classification can be used to classify galaxies into simple early/spiral/peculiar bins in the HDF-N. But at $I_{814W} \sim 25$ mag photometric redshifts studies (eg. Sawicki, Lin, & Yee 1997; Wang et al 1998; Hogg et al 1998) indicate serious contamination by very high-redshift spirals, and it is likely that bars are undetectable due to both bandshifting of the rest frame and low signal-to-noise. Although such effects can be calibrated by simulations, without deep images probing rest-frame optical wavelengths at high redshifts, the validity of such simulations is difficult to assess. A more robust test would restrict samples to low-inclination spirals with redshifts less than $z \sim 1$, where bandshifting effects are negligible and where signal-to-noise levels are high enough for unambiguous bar detection. Until the release of the southern Hubble Deep Field (HDF-S), no adequately large deep imaging sample has been available.

A final complication is that the fraction of *local* barred spirals remains controversial. There is a continuum in apparent bar strength in galaxies, and the strength required to merit classification as a barred galaxy is highly subjective.

For example, there is reasonable agreement in local catalogues that the proportion of *strongly* barred galaxies is 25%–35%, based on the numbers given in the *Revised Shapley-Ames Catalogue* (RSA; Sandage & Tammann 1987), the *Third Reference Catalogue* (RC3; de Vaucouleurs et al. 1991), and the *Uppsala General Catalogue* (UGC; Nilson 1973). However an additional 30% of spirals are classed as *weakly* barred in the RC3, substantially higher than in the UGC or RSA. Quite apart from taxonomical differences in accounting for weakly barred systems, morphological classifications at low redshift have largely been based on subjective inspections of photographic data with limited dynamic range, leading to poor agreement in the classifications made by observers using the same classification system (Naim et al. 1995).

In the present paper we demonstrate how these difficulties can be surmounted through quantitative measures of bar strength for a large sample of spiral galaxies culled from both Hubble Deep Fields. It is clear that since the proportion of locally barred spirals is poorly defined, the optimal way to probe for evolution in the bar fraction is an objective study that encompasses internally a broad range of redshifts. The recent release of the HDF-S has doubled the size of a suitably deep sample and has motivated the current analysis. A plan of the paper follows. In Section 2 we describe our objective measure of bar strength, outline its physical significance, and show how this bar-strength measure has been calibrated using local galaxy samples. In Section 3 we demonstrate the robustness of our bar strength parameter, and calculate the limits to which strongly barred systems should be detectable in the Hubble Deep Fields. The methodology from Abraham et al (1996) is used to select from the HDF samples a subset of low-inclination spirals whose images have sufficient signal-to-noise to allow barred structure to be detected. We then determine the fraction of barred galaxies in the Northern and Southern Hubble Deep Fields as a function of spectroscopic and photometric redshift, and conclude that a strong evolutionary effect exists. In Section 4 we discuss the implications (and associated uncertainties) of our results for models of the formation of bars, bulges, and disks at high redshifts. Our conclusions are summarised in Section 5.

2 A QUANTITATIVE MEASURE OF BAR STRENGTH

2.1 Methodology

Characterising spiral structure in distant systems poses a challenge because of the diversity of arm structures that are seen locally, and because spiral arms can be difficult to observe at low signal-to-noise levels where surface brightness dimming becomes important. However, in the absence of strong bandshifting effects (the importance of which are discussed in §2.2), galactic bars should be the easiest of the spiral features to detect in high resolution data because of their inherent brightness and symmetry about the central nucleus.

The presence of a bar in a galaxy will have two measurable effects on its photometry: generally speaking, the ellipticity of the isophotes will change between the region of the bar and the outer galaxy, and the principal axes of the

isophotes will also vary between these two regions. In order to quantify the strength of these signatures in distant galaxies, we have adopted the following procedure. Galaxy images are first isolated from the sky background by extracting contiguous pixels at 1.5σ above the sky level. Each galaxy image is then “sliced” at 1% and 85% of its maximum flux level. The second-order moments of the pixels brighter than these flux thresholds define two best-fitting ellipses, the first for the entire galaxy and the second for the inner portion of the galaxy near the nucleus. From the parameters of these best-fit ellipses, we extract the axis ratio of the galaxy as a whole, $(b/a)_{\text{outer}}$, and that of the inner part of the galaxy, $(b/a)_{\text{inner}}$. We also measure the twist angle between the principle axes of these ellipses, $\phi = \phi_{85\%}$ ($0 < \phi < 90^\circ$).

In the vast majority of cases, the cut at 85% of the maximum flux proves an effective level for isolating any bar-like structures. However, in a few obviously-barred galaxies with bright nuclei (often systems with dominant rings, “fat” bars, or morphological lenses) this cut lies inside the strongly-barred region. We therefore repeat the analysis with the inner cut at a flux level of 50% of the maximum. If this choice of flux level were to detect a bar that the original choice missed, then we would expect the twist between the ellipses in this analysis, $\phi_{50\%}$, to be much greater than $\phi_{85\%}$. Therefore, if $\phi_{50\%} > 10 \times \phi_{85\%}$, then we adopt this lower flux cut to determine $(b/a)_{\text{inner}}$, and define the twist angle by $\phi = \phi_{50\%}$.

We now need some objective criterion for interpreting the measured values of $(b/a)_{\text{inner}}$, $(b/a)_{\text{outer}}$ and ϕ as a measure of the “barriness” of a galaxy. To do so, we have chosen to measure a parameter related to *the physical axial ratio of the bar* in an idealized galaxy. Consider a simple model for a galaxy in which at large radii it is an axisymmetric thin disk, so that its inclination, i , is directly related to $(b/a)_{\text{outer}}$:

$$i = \cos^{-1}[(b/a)_{\text{outer}}]. \quad (1)$$

If we further assume that the inner region quantified by $(b/a)_{\text{inner}}$ can be modelled by an elliptical distribution of light lying in the same plane as the outer disk, then we can infer its intrinsic axis ratio, $(b/a)_{\text{bar}}$, from the measured values of $(b/a)_{\text{inner}}$, ϕ , and i . After the appropriate coordinate transformations have been made to rotate the galaxy to face-on, we find that

$$(b/a)_{\text{bar}}^2 = \frac{1}{2} \left(X - \sqrt{X^2 - 4} \right), \quad (2)$$

where

$$\begin{aligned} X = & \sec^2 i \left[2 \cos^2 \phi \sin^2 \phi \sin^4 i \right. \\ & + (b/a)_{\text{inner}}^2 (1 - \sin^2 \phi \sin^2 i)^2 \\ & \left. + (b/a)_{\text{inner}}^{-2} (1 - \cos^2 \phi \sin^2 i)^2 \right]. \end{aligned} \quad (3)$$

Formally, these formulae only yield the axis ratio for a bar in the idealized case where it is flat, exactly elliptical, and embedded in a circular disk. However, as we will show in the next section, the value of $(b/a)_{\text{bar}}^2$ still provides a robust, objective measure of “barriness” when these ideal conditions are relaxed: real galaxies that the eye recognizes as barred have systematically larger values of $(b/a)_{\text{bar}}^2$ than do unbarred systems. There is, however, one important caveat to the general applicability of this formula: the assumption of a two-dimensional disk clearly becomes unreasonable if a galaxy is viewed close to edge-on, when the three-

dimensional shape of the central bulge becomes a prominent feature. However, it is intrinsically almost impossible to determine whether a galaxy that lies close to edge-on is barred on the basis of photometry alone. We therefore only attempt to determine the value of $(b/a)_{\text{bar}}^2$ for galaxies where we derive an inclination of $i < 60$ degrees.

2.2 Calibration

As we will review in §3, our expectation (based on nearly complete redshift information from the Northern HDF, and photometric redshifts in the Southern HDF) is that $> 90\%$ of spirals in the HDF samples at $I_{814W} < 23$ mag lie at redshifts $z < 1$. We argue in this section that this magnitude limit is also approximately that at which bars are generally detectable in HDF WF/PC2 images on the basis of signal-to-noise. The importance of these two statements is that local B -band images represent a close rest-frame match to most of the distant spirals in an $I_{814W} < 23$ mag HDF sample*. In other words, our study will be largely unaffected by “morphological K-corrections” that play a significant role in the interpretation of HDF data at $I_{814W} > 23$ mag.

The effective B -band rest wavelength of most of our sample is also convenient because of the public availability of a sample of B -band CCD data for a “generic” sample of bright local galaxies (Frei et al. 1996). The Frei sample of local galaxies was observed at a physical resolution similar to that achieved by HST when probing high-redshift galaxies. This sample can therefore be used in order to investigate the utility of $(b/a)_{\text{bar}}^2$ in discriminating between barred and unbarred spirals.

Measurements of $(b/a)_{\text{bar}}^2$ for all spiral galaxies in the Frei et al. (1996) sample are shown in Figure 1. (In this figure, and throughout the remainder of this paper we will adopt the terminology of the RC3, and denote strongly barred spirals as class SB, weakly/tentatively barred systems as class SAB, and unbarred spirals as class SA.) It is clear that the single $(b/a)_{\text{bar}}^2$ parameter is remarkably effective at distinguishing between strongly barred and unbarred spiral systems. A representative cut in $(b/a)_{\text{bar}}^2$ useful for discriminating between strongly barred and non-barred samples is $(b/a)_{\text{bar}}^2 = 0.45$. At all inclinations SB galaxies have systematically smaller $(b/a)_{\text{bar}}^2$ than SA systems, although the gulf between the two classes is a fairly strong function of inclination, and by $i \sim 70$ degrees the classes are sufficiently intermingled that our methodology is rendered ineffective. As described in §2.1 this is entirely expected because of the difficulty in distinguishing highly in-

* In fact, for many of the brighter HDF galaxies studied in the present paper, local B -band calibration data is actually somewhat *blueward* of the observed rest wavelengths for HDF galaxies. However, in local galaxies, bars are not substantially more visible at rest V -band wavelengths, compared to rest B -band. We have confirmed this by duplicating the present analysis with R -band images of galaxies in the Frei et al. (1996) sample, in which we find a very similar distribution to that shown in Figure 1. Bar visibility is expected to drop off markedly blueward of the 4000Å break, and to increase sharply in the near infrared for most red bars, because of the strong suppression in the visibility of young stellar populations, enhancing the relative contrast of the generally reddish bars relative to the disc.

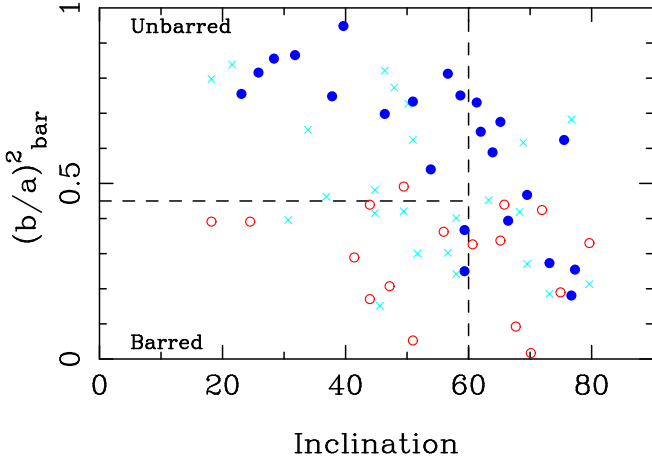


Figure 1. $(b/a)_{\text{bar}}^2$ plotted as a function of galaxy inclination for the local spirals in the Frei et al. (1996) B-band CCD imaging sample. Note how this single parameter is remarkably effective at distinguishing between barred and unbarred spirals at inclinations below ~ 60 degrees. Both our proposed cut at $(b/a)_{\text{bar}}^2 = 0.45$ and inclination cut at 60 degrees are shown. Symbols are keyed to classifications in RC3. Strongly barred spirals (RC3 class SB) are shown as open circles, weakly barred spirals (RC3 class SAB) are shown as crosses, and unbarred spirals (RC3 class SA) are shown as filled circles.

clined barred from unbarred spirals, not only in our objective analysis, but also when undertaking visual classifications (Naim et al. 1995). SAB systems typically lie in-between the strongly and weakly barred systems at any given inclination. In the present paper we adopt an inclination limit of 60 degrees in defining our sample. Our methodology does not distinguish the tentative/weakly barred SAB systems from other classes, but as described earlier there is good evidence that visual classification of these systems is particularly subjective and inherently rather poorly defined in local catalogs (Naim et al. 1995).

3 BARRED GALAXIES IN THE HUBBLE DEEP FIELDS

We now proceed to discuss the application of the $(b/a)_{\text{bar}}^2$ parameter in the measurement the bar fraction in the Hubble Deep Fields. Adopting the formulation described in Abraham et al. (1996a,b), the Frei et al. (1996) sample was artificially redshifted within the range $0 < z < 1.5$ in order to determine the faintest magnitude to which $(b/a)_{\text{bar}}^2$ can be determined accurately under the conditions of the HDFs. The very clean separation between SA and SB systems in Figure 1 was recovered to synthetic redshifts associated with $I_{814W} = 23.2$ mag, which we adopted as our magnitude limit. This limit was subsequently confirmed by an internal analysis of data from the HDFs themselves. In this procedure, bright spirals in the HDFs were shrunk, faded, convolved with the PSF, noise-degraded and digitally added to blank portions of the HDF-North in order to test the magnitude limit at a range of isophotal sizes spanning the observed size distribution of $I_{814W} \sim 23$ mag spirals. The robustness of $(b/a)_{\text{bar}}^2$ at our adopted I_{814W} magnitude limit is shown in Figure 2.

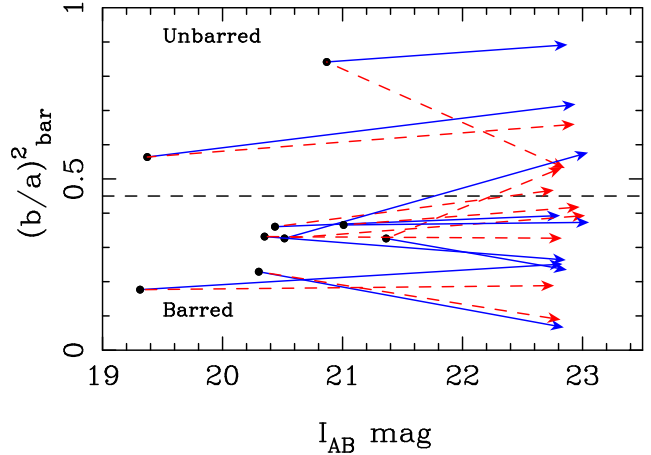


Figure 2. Tracks showing the recovery of $(b/a)_{\text{bar}}^2$ measurements for bright HDF systems degraded to the magnitude limit of our sample. The predominantly horizontal tracks indicate that, within the range explored in the present paper, measurements of $(b/a)_{\text{bar}}^2$ are robust to signal-to-noise and size degradation. Solid tracks correspond to galaxies reduced to 60% of their original size, and dashed tracks to the galaxies in the extreme case where galaxies are reduced to 30% of their original size. After size reduction and diminution of galaxian light to our approximate flux limit, galaxies were convolved with the dithered HST I_{814W} -band PSF before being digitally added to a blank portion of the HDF sky and re-analysed.

Prior to measuring $(b/a)_{\text{bar}}^2$, spiral systems were extracted from the galaxy mix using the Abraham et al (1996a) asymmetry-concentration (A-C) classifier.[†] The previously mentioned inclination cut of $i < 60^\circ$ was then applied, resulting in a low-inclination sample of 20 HDF-N and 28 HDF-S spiral galaxies of which 18 (35%) are strongly barred (9 in each HDF) according to the $(b/a)_{\text{bar}}^2$ discriminator described in Section 2.2. A montage of these galaxies is presented in Figure 3.

Subsequent visual inspection of these images indicates a possible uncertainty in the barred identification of, at most, four systems. In two, features identified as a weak spiral arm emanating from a bar could conceivably be a companion or optically superposed galaxy aligned at right angles to the main body of the galaxy, leading to a spurious classification. In one case, a strong bar is clearly seen, but it is not obviously accompanied by spiral structure in the outer regions, making classification as a peculiar possibly appropriate. In the final case, the inner isophotal structure could be described as perhaps more lens-like than bar-like. (Similar systems are sometimes categorized as barred in local catalogues – the distinction between nuclear bars and lenses can be rather subjective). Each of these uncertainties would diminish the proportion of barred spirals at $z \simeq 0.5$ and not affect the overall conclusion of the paper.

A more important question is whether, in selecting the face-on spiral sample using the A-C estimator, some barred

[†] The morphological region used to extract spirals in the log A vs. log C classification plane was defined in terms of linear boundaries, as in Abraham et al (1996a). Both the early-type vs. spiral and spiral vs. irr/peculiar/merger lines intersect the $\log(A)=0$ axis at $\log(C)=-0.16$, with slopes of 9.15 and 2.30, respectively.

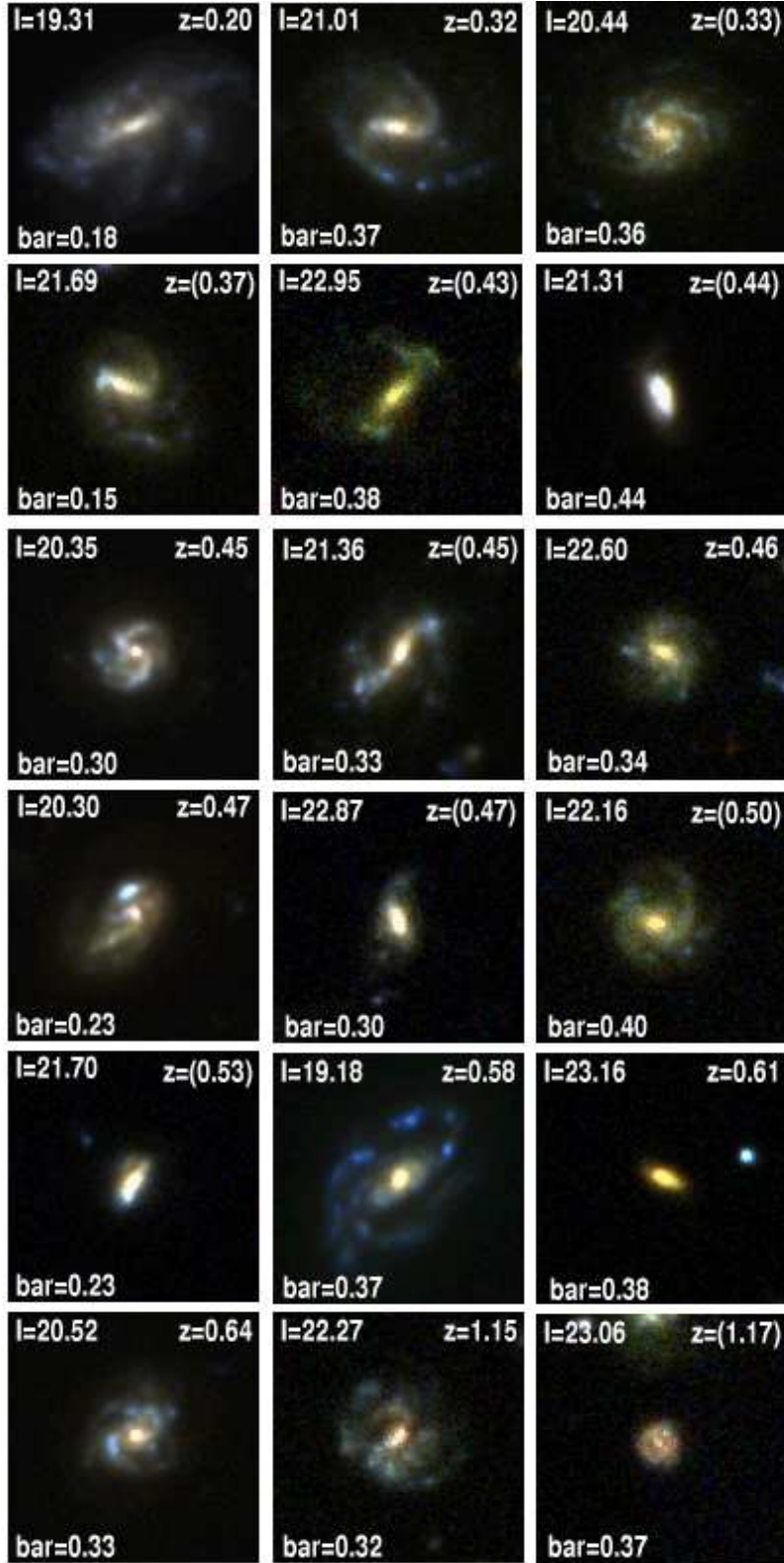


Figure 3. All spiral galaxies with $I_{814W} < 23.2$, inclination $i < 60^\circ$ and $(b/a)_{\text{bar}}^2 < 0.45$ in the northern and southern Hubble Deep Fields ordered according to redshift. True colour images are shown, constructed from the B_{450W} , V_{814W} , and I_{814W} -band data. Each panel represents a field of 5.1 arcsec on a side. The redshift and value of $(b/a)_{\text{bar}}^2$ is indicated (photometric redshifts are in parenthesis).

objects have been missed. This would be immaterial in estimating the fraction of barred/unbarred galaxies in the HDF unless, by some means, barred systems were preferentially excluded in extracting the A-C spiral sample. We have investigated this by visually classifying all galaxies in the HDF-S/N to $I_{814}=23.2$ mag. As in Abraham et al (1996a,b), the agreement between the A-C spiral selection and the visual spiral selection was excellent. Visual classification would add two barred spirals to the montage shown in Figure 3, and as both systems are bright and at low redshift, inclusion of these objects would actually slightly strengthen the conclusions of this paper.

As described in the Introduction, because of disagreements with regard to the definitions and proportions of weakly-barred spirals in local catalogues, one cannot robustly map the $(b/a)_{\text{bar}}^2$ discriminator onto the SA/SAB/SB scheme to compare with the local barred spiral fraction. Therefore a more productive way forward is a *self-consistent internal comparison of the redshift distribution of barred and unbarred spirals within the HDF datasets*. In order to construct this for our magnitude-limited sample, we must augment the spectroscopic redshifts available for the HDFs with photometric redshift estimates, particularly for HDF-S for which published spectroscopic data is limited. In the HDF-N all but two systems in our sample have known spectroscopic redshifts, while in the HDF-S the situation is almost exactly reversed, with only two galaxies in our sample having currently known spectroscopic redshifts (Glazebrook et al. 1998, in preparation). As barred spirals are indistinguishable from their non-barred counterparts on the basis of colour (de Vaucouleurs 1961) we do not expect errors in the determination of photometric redshifts to significantly bias our results.

In the case of the HDF-N, we used the compilation of Wang et al (1998) to provide photometric redshifts for the 2 remaining HDF-N face-on spirals to $I_{814}=23.2$ without spectroscopic data. For the HDF-S sample we have computed our own photometric redshifts, based on a template fitting method (Brinchmann et al 1998, in preparation) similar to that used by Fernández-Soto et al (1998). We have compared our estimates in the HDF-N with those obtained using the linear fitting formulae from Wang et al (1998). Our determinations agree well with a negligible mean offset and an RMS scatter of only 0.1 in redshift, which is adequate for our purposes. Both methods have been extensively tested against spectroscopic data in the HDF-N (Wang et al 1998) and within the redshift range concerned agree remarkably well.

Figure 4 shows the redshift distribution of barred and unbarred spirals in the Hubble Deep Fields North and South. *This diagram reveals a striking decline in the proportion of barred examples beyond a redshift $z \sim 0.5$.* This cannot be due to uncertainties in using photometric redshifts for the HDF-S as the same effect is seen in both HDF samples and the HDF-N is spectroscopically complete at the 90% level. Formally, the redshift distributions of the barred and unbarred samples selected on the basis of $(b/a)_{\text{bar}}^2$ are inconsistent at the 99.8% confidence level from a Kolmogorov-Smirnov test. We conclude that Figure 4 shows strong evidence for differential evolution in the abundance of barred spirals at high redshift, in the sense of a marked decrease in the proportion of barred spirals beyond $z \simeq 0.5$.

4 DISCUSSION

As mentioned in the Introduction, there are two basic criteria that must be met for the bar-forming instability to be effective: the material in the disk must be self-gravitating, and it must be following relatively well-ordered orbits, without excessive random motion. Thus, one possible explanation for the deficit of barred galaxies beyond $z \sim 0.5$ is that disks at these redshifts have not yet accreted sufficient material to be self-gravitating. Unfortunately, it is difficult to measure the degree to which the masses of disks dominate even in nearby galaxies with plentiful kinematic data (e.g. Casertano & van Albada 1990, Freeman 1993, van der Kruit 1995), so it will be very hard to test this hypothesis observationally on these high-redshift objects.

The second possibility is that the bar instability is suppressed due to larger random motions in the material making up the high-redshift disks (e.g. Ostriker & Peebles 1973). If a disk has only recently formed, one might expect the orbits of the material in it to reflect the somewhat stochastic process by which it was assembled, leading to relatively large random components in their motion. Such a “hot” disk would prove resistant to the bar instability, explaining the deficit of barred galaxies at higher redshifts.

A final possibility is that the mechanisms that destroy bars are more efficient at high redshift. For example, Pfenniger (1991) has shown that a merger with a compact companion can heat a disk to a point where any bar is destroyed; a more major merger, on the other hand, would entirely destroy the disk, leaving an elliptical galaxy (e.g. Barnes 1992). In any hierarchical picture of galaxy formation, mergers are more common at high redshift, and generally consist of collisions with less-developed small galaxies (Navarro, Frenk & White 1994). We would therefore expect a higher rate of conversion of barred galaxies into unbarred disk galaxies at high redshift than we see today.

The efficient suppression of a high-redshift bar may not even require the intervention of an outside agency such as a merger. As discussed in the Introduction, bars are known to be unstable entities, which evolve into spheroidal bulge-like structures. This spontaneous buckling process introduces a random element into the motions of stars similar to that induced by a minor merger, and so acts to suppress subsequent bar formation. In an internal-colour based analysis of bright HDF-N galaxies (Abraham et al. 1999), it was concluded that high-redshift bulges are the oldest components of the galaxies at the epoch of observation. If these bulges formed from an early generation of bars at a redshift higher than that probed in the present study, then further bar formation will be inhibited until sufficient new material has been added to the disk on well-ordered orbits to allow the instability to act. Thus, the deficit of barred systems at $z > 0.5$ may represent a temporary lull in the phenomenon while the galaxies recover from their first bout of bar formation.

Similarly, Hasan & Norman (1990) have shown that the presence of a central mass of a few percent of the total disk mass will suppress the bar-forming instability. In addition, a bar provides an effective mechanism for channeling gas toward the centre of a galaxy (e.g. Friedli & Benz 1993). Thus, we might expect a bar to eventually destroy itself by feeding sufficient material toward the centre of its galaxy to suppress the instability. Sellwood & Moore (1998) have

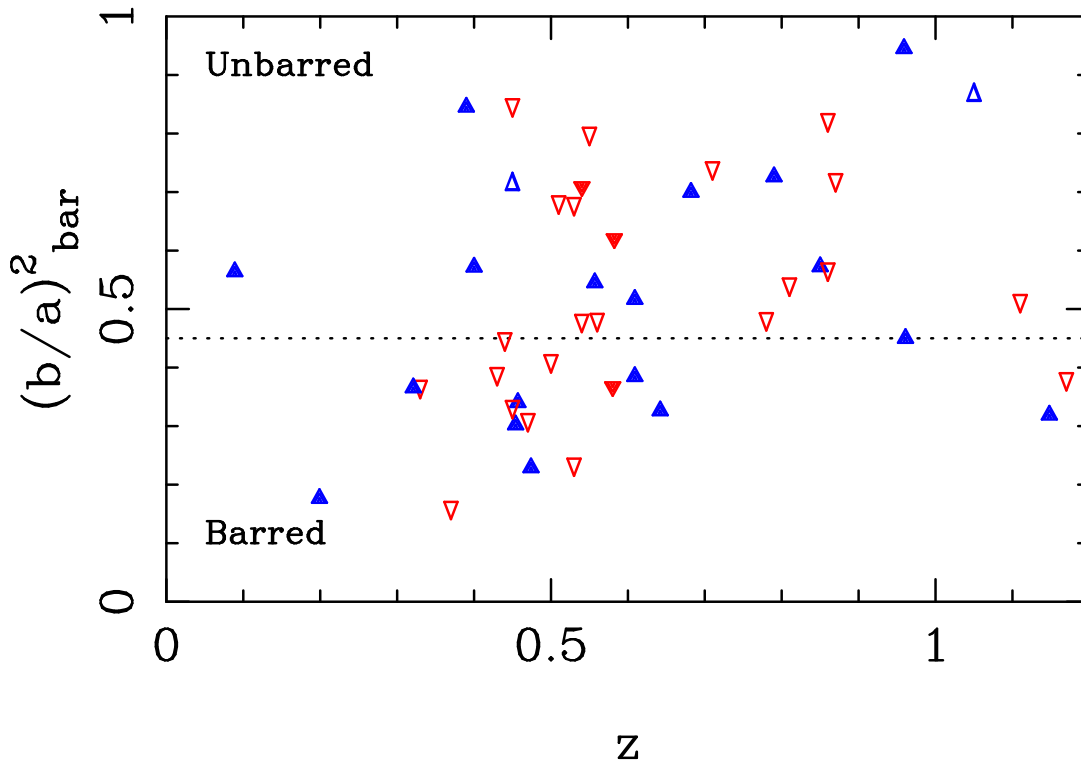


Figure 4. The bar strength estimator $(b/a)_{\text{bar}}^2$ plotted as a function of spectroscopic redshift (filled symbols) or photometric redshift (open symbols) in the northern (triangles pointing upward) and southern (triangles pointing downward) Hubble Deep Fields. Note the marked gradient in the proportion of barred systems with redshift, beginning at $z \sim 0.5 - 0.6$.

explored this scenario in some detail, and have pointed out that several mechanisms exist by which a second generation bar could be produced, perhaps explaining the prevalence of bars at low redshifts.

5 CONCLUSIONS

We have defined a simple measure of bar strength suitable for probing the internal structure of faint galaxies. Our technique is based on measuring parameters sensitive to the photometric signatures of barred spiral structure. These observables can be combined to yield the *physical* axial ratio of a bar, under the assumption of an elliptical bar embedded within a round, thin disk. Where these assumptions are not a good approximation, the estimator still yields a perfectly quantitative, objective parameter that appears to closely track visual estimates of bar strength.

Our parametric bar estimator, $(b/a)_{\text{bar}}^2$, has been tested against local samples of spirals, and against artificially redshifted spirals under the conditions of the Hubble Deep Fields. For reasonably low-inclination systems (< 60 degrees), spirals classed locally as SA are cleanly-separated from systems classed as SB. We demonstrate that distinguishing between barred and unbarred spirals on the basis of $(b/a)_{\text{bar}}^2$ is possible to $I = 23.2$ in the Hubble Deep Fields.

The release of the Southern Hubble Deep Field has increased the sample of $I < 23$ mag low-inclination galaxies substantially, allowing the first detailed investigation of redshift evolution in the barred spiral fraction. By combining measurements of $(b/a)_{\text{bar}}^2$ with spectroscopic and photomet-

ric redshifts in the Hubble Deep Fields, a striking decrease in the proportion of barred spirals as a function of redshift beyond $z = 0.5$ has been discovered. Our result supports the observation by van den Bergh et al. (1996) that barred spirals are deficient at faint magnitudes in the northern HDF.

The physical mechanisms responsible for the absence of barred spirals at high redshifts is unclear. Possibilities we have discussed include dynamically hotter (or increasingly dark-matter dominated) high-redshift discs, and an enhanced efficiency in bar destruction at high redshifts. For all these scenarios, the present result provides a clear observational benchmark. Our investigation has brought forward the epoch at which the conventional Hubble system is observed to be in place, from $z \sim 1$ (based on the the abundance of morphologically peculiar systems in the LDSS/CFRS redshift survey described in Brinchmann et al. 1988) to $z \sim 0.5$.

Acknowledgments We thank Bob Williams and Harry Ferguson at STScI for their encouragement, and the entire STScI for their heroic efforts in releasing the HDF-S data promptly as advertised. We also thank Alar Toomre, Len Cowie, Malcolm Longair and Sidney van den Bergh for useful discussions. RGA and MM acknowledge PPARC for support under the Advanced Fellowship programme. JB acknowledges receipt of an Isaac Newton Studentship.

REFERENCES

- Abraham, R. G., Tanvir, N. R., Santiago, B. X., Ellis, R. S., Glazebrook, K., van den Bergh, S. 1996a, MNRAS, 279, L47
- Abraham, R. G., van den Bergh, S., Ellis, R. S., Glazebrook, K., Santiago, B. X., Griffiths, R. E., Surma, P. 1996b, ApJS, 107, 1
- Abraham, R. G., Ellis, R. S., Fabian, A. C., Tanvir, N. R. & Glazebrook, K., 1998, MNRAS, in press, (astro-ph/9807140)
- Barnes, J.E., 1992, ApJ, 393, 484
- Brinchmann, J., Abraham, R. G., Schade, D., Tresse, L., Ellis, R. S., Lilly, S. J., Le Fevre, O., Glazebrook, K., Hammer, F., Colless, M., Crampton, D., & Broadhurst, T. 1998, ApJ, 500, 75.
- Casertano, S. & van Albada, T.S., 1990, in Bayonic Dark Matter, eds D. Lynden-Bell & G. Gilmore (Dordrecht: Kluwer), 159
- Combes, F., Debbasch, F., Friedli, D., Pfeffinger, D. 1990, A&A, 233, 82
- Cowie, L. L., Songaila, A., Hu, E. M., Cohen, J. G. 1996, AJ, 112, 839
- de Vaucouleurs, G., 1961, AJ, 66, 629
- de Vaucouleurs, G., de Vaucouleurs, A., Corwin, H.G., Buta, R.J., Paturel, G. & Fouqu'e, P., 1991, Third Reference Catalogue of Bright Galaxies (New York: Springer-Verlag)
- Driver, S. P., Windhorst, R. A., Griffiths, R. E. 1995a, ApJ, 453, 48
- Driver, S. P., Fernandez-Soto, A., Couch, W. J., Odewahn, S. C., Windhorst, R. A., Lanzetta, K., & Yahil, K. 1998 (ApJ(Letters), in press, astro-ph/9802092)
- Eggen, O., Lynden-Bell, D., & Sandage, A. 1962, ApJ, 136, 748
- Ellis, R. S. 1998 Nature, 395, A3
- Fernández-Soto, A., Lanzetta, K. M., Yahil, A. astro-ph/9809126
- Freeman, K.C., 1993, in Physics of Nearby Galaxies: Nature or Nurture? eds R.X. Thuan, C. Balkowski & J. Thanh Van (Paris: Edition Frontières), 201
- Frei, Z., Guhathakurta, P., Gunn, J.E., Tyson, J.A., 1996, AJ, 111, 174
- Friedli, D. & Benz, W., 1993, A&A, 268, 65
- Glazebrook, K., Ellis, R., Santiago, B., Griffiths, R. 1995, MNRAS, 275, L19
- Hasan, H. & Norman, C., 1990, ApJ, 361, 69
- Hogg, D. et al. 1998, AJ, 115, 1418
- Marleau, F. R. & Simard, L. 1998, ApJ, 507, 585
- Miller, R.H., Prendergast, K.H., & Quirk, W.J. 1970, ApJ, 161, 903
- Naim, A. Lahav, O., Buta, R.J., Corwin, H.G., de Vaucouleurs, G., Dressler, A., Huchra, J.P., van den Bergh, S., Raychaudhury, S., Sodre, L., Storrie-Lombardi, M.C., 1995, MNRAS, 274, 1107
- Navarro, J.F., Frenk, C.S. & White, S.D.M., 1994, MNRAS, 267, L1.
- Nilson, P. 1973. *Uppsala General Catalogue of Galaxies*, Acta Upsaliensis Ser V: A Vol I
- Norman, C. A., Sellwood, J. A., & Hasan, H. 1996, ApJ, 462, 114
- Odewahn, S. C., Windhorst, R. A., Driver, S. P., Keel, W. C. 1996, ApJL, 472, L13
- Ostriker, J.P. & Peebles, P.J.E., 1993, ApJ, 186, 467
- Pfenniger, D., 1991, in Dynamics of Disk Galaxies, ed. B. Sundelius (Göteborg: Göteborgs University), 191
- Quillen, A., 1998, in Galaxy Dynamics, eds D. Merritt, M. Valuri & J. Sellwood, ASP, in press.
- Quillen, A. & Sarajedini, V. L., 1998, AJ, 115, 1412.
- Raha, N., Sellwood, J.A., James, R.A., Kahn, F.D., 1991, Nature, 352, 411
- Sandage, A. & Tammann, G.A., 1987, A Revised Shapley-Ames Catalog of Bright Galaxies (Carnegie Institute of Washington)
- Sawicki, M., Lin, H., & Yee, H. K. C. 1997, AJ, 113, 1
- Schade, D., Lilly, S. J., Crampton, D., Hammer, F., Le Fevre, O., Tresse, L. 1995, ApJl, 451, L1
- Sellwood, J.A. & Moore, E.M, 1998, ApJ, in press (astro-ph/9807010)
- Smail, I., Hogg, D. W., Yan, L., & Cohen, J., ApJ, 449, 105.
- van den Bergh, S., Abraham, R. G., Ellis, R. S., Tanvir, N. R., Santiago, B. X. 1996, AJ, 112, 359.
- van der Kruit, P.C., 1995, in IAU Symp. 164, Stellar Populations, Eds. P.C. van der Kruit & G. Gilmore (Dordrecht: Kluwer), 205
- Wang, Y., Bahcall, N., Turner, E. L., 1998, AJ, 116, 2081
- Williams et al. 1996, AJ, 112, 1335

This figure "bar_mosaic.jpg" is available in "jpg" format from:

<http://arxiv.org/ps/astro-ph/9811476v1>